Dynamic Downscaling of Seasonal Simulations over South America

VASUBANDHU MISRA, PAUL A. DIRMEYER, AND BEN P. KIRTMAN

Center for Ocean–Land–Atmosphere Studies, Institute of Global Environment and Society, Inc., Calverton, Maryland

(Manuscript received 13 August 2001, in final form 24 June 2002)

ABSTRACT

In this paper multiple atmospheric global circulation model (AGCM) integrations at T42 spectral truncation and prescribed sea surface temperature were used to drive regional spectral model (RSM) simulations at 80-km resolution for the austral summer season (January–February–March). Relative to the AGCM, the RSM improves the ensemble mean simulation of precipitation and the lower- and upper-level tropospheric circulation over both tropical and subtropical South America and the neighboring ocean basins. It is also seen that the RSM exacerbates the dry bias over the northern tip of South America and the Nordeste region, and perpetuates the erroneous split intertropical convergence zone (ITCZ) over both the Pacific and Atlantic Ocean basins from the AGCM. The RSM at 80-km horizontal resolution is able to reasonably resolve the Altiplano plateau. This led to an improvement in the mean precipitation over the plateau. The improved resolution orography in the RSM did not substantially change the predictability of the precipitation, surface fluxes, or upper- and lower-level winds in the vicinity of the Andes Mountains from the AGCM. In spite of identical convective and land surface parameterization schemes, the diagnostic quantities, such as precipitation and surface fluxes, show significant differences in the intramodel variability over oceans and certain parts of the Amazon River basin (ARB). However, the prognostic variables of the models exhibit relatively similar model noise structures and magnitude. This suggests that the model physics are in large part responsible for the divergence of the solutions in the two models. However, the surface temperature and fluxes from the land surface scheme of the model [Simplified Simple Biosphere scheme (SSiB)] display comparable intramodel variability, except over certain parts of ARB in the two models. This suggests a certain resilience of predictability in SSiB (over the chosen domain of study) to variations in horizontal resolution. It is seen in this study that the summer precipitation over tropical and subtropical South America is highly unpredictable in both models.

1. Introduction

The present generation of atmospheric global circulation models (AGCMs) used for seasonal simulations and predictions are limited in their use for many smaller-scale applications because of their coarse horizontal resolution. The poor reliability of their high-frequency features renders it difficult to use them for examining regional-scale variability. Computing resources limit the use of very high-resolution AGCMs for ensemble seasonal predictions. As a result, the community has resorted to either statistical or dynamical downscaling in order to predict the regional-scale variability. However, the superiority of one approach over the other is not clearly established (Wilby and Wigley 1997). In this paper, we pursue the latter approach of dynamical downscaling. This approach involves a regional climate model, in this case the regional spectral model (RSM; Juang et al. 1997). The RSM is forced at the lateral boundaries by the AGCM. Under this configuration the AGCM generates the large-scale atmospheric forcing for the regional domain while the regional model resolves the sub-AGCM grid-scale response. The successful results of the works of Giorgi (1990) over the western United States, Ji and Vernekar (1997) over Indian monsoons, Tanajura (1996) over the South American region, and Fennessy and Shukla (2000) over North America have already provided the scientific justification of this procedure.

The main source for understanding South American climate has been diagnostic studies from reanalyses and observations (Rao et al. 2002; Marengo et al. 2001). The results from climate model integrations over this region are relatively few. This study, in addition to showing the results from downscaling seasonal simulations, also highlights the capabilities and shortcomings of modeling seasonal climate variability over the South American region from a state-of-the-art AGCM.

Climate modeling studies over South America (Nigam and DeWeaver 1998; Figueroa et al. 1995) have shown that the Andes Mountains strongly influence the low-level circulation in the region and is primarily responsible for the transport of moisture from the Amazon

Corresponding author address: Dr. Vasubandhu Misra, Center for Ocean–Land–Atmosphere Studies, Institute for Global Environment and Society, Inc., 4041 Powder Mill Road, Suite 302, Calverton, MD 20705.
E-mail: misra@cola.iges.org

River basin to the subtropical latitudes of South America through the low-level jet. Furthermore, Nigam and DeWeaver (1998) show that secondary orographic interactions are important in generating extratropical circulation anomalies in response to tropical heating anomalies. In high-resolution models, these topographic features and the associated circulations are better resolved. In a related downscaling study, Chou et al. (2000) show that the improvement in the monthly mean forecast over South America from the regional model is more significant in the austral dry months than in the austral wet months. They attribute this behavior to the shortcomings of their simplified land surface and convection schemes. In another regional modeling study over the South America region Menendez et al. (2001) find that in the austral winter season both the AGCM and the regional model have similar systematic errors but the biases are reduced in the higher-resolution model simulation.

Earlier studies (Misra et al. 2002a,b) have shown that over South America the RSM at 80-km horizontal resolution improves the simulation compared to the coarser National Centers for Environmental Prediction (NCEP) reanalysis at approximately 1.9° resolution. This was confirmed by comparing the independent outgoing longwave radiation dataset of Liebmann and Smith (1996) with those from NCEP reanalysis and RSM regional climate simulations. In this paper we examine RSM simulations forced at the lateral boundaries by an AGCM rather than by reanalyses. The solutions from the two models (RSM and AGCM) are compared over the South American continental region and over the neighboring ocean basins.

Geophysical fluid dynamics are inherently nonlinear. Hence, predictability in an atmospheric model or the real atmosphere is limited to two weeks or less. As a result of the nonlinearities, small differences in the initial state between two simulations of an AGCM will quickly grow and propagate globally. For monthly or seasonal climate investigations, statistical stability and improved skill in simulation of the mean is achieved by averaging an ensemble of such integrations, where each ensemble member has a perturbed initial condition (Leith 1974).

In a regional model, the lateral boundaries are prescribed. If the source of the lateral boundary conditions come from an AGCM integration, the large-scale features of the regional model will not diverge considerably from that of the AGCM. On smaller scales, some internal variability is generated that differs from the AGCM state, because of differences in resolution and physical parameterizations in the regional model. These differences are worthwhile to analyze, as they may modulate the underlying large-scale signal (Giorgi and Bi 2000). Likewise, an ensemble of regional model integrations with specified lateral boundary conditions from separate members of an AGCM ensemble simulation will show enhanced intraensemble variability. In this study, we examine the ensemble spread (model noise) of the regional and global models.

In the following section we briefly describe the two models used in this study followed by a description of the design of the experiments in section 3. The ensemble means of the two models are compared in section 4 and the ensemble spread in the two models is presented in section 5. Finally conclusions are made in section 6.

2. Model description

The AGCM used in this study is version 2.2 of the Center for Ocean–Land–Atmosphere Studies (COLA) global spectral model (T42,L18). This version of the model has the dynamical core of the National Center for Atmospheric Research (NCAR) Community Climate Model version 3 (CCM3) described in Kiehl et al. (1998). Additional details can be found in Schneider (2001). All the dependent variables are spectrally treated except the moisture variable, which, is advected using the semi-Lagrangian technique. For a full description of the COLA AGCM physics package the readers are directed to Kinter et al. (1997). A brief outline of the COLA physics is presented here:

- Shortwave radiation: Lacis and Hansen (1974), Davies (1982);
- Longwave radiation: Harshvardhan et al. (1987);
- Boundary layer scheme: Miyakoda and Sirutis (1977);
- Vertical diffusion: Mellor and Yamada (1982);
- Deep convection scheme: Relaxed Arakawa–Schubert (RAS) scheme, Moorthi and Suarez (1992);
- Shallow convection: Tiedtke (1984);
- Gravity wave drag parameterization: Alpert et al. (1988);
- Land surface processes: Simplified Simple Biosphere scheme (SSiB) of Dirmeyer and Zeng (1997);
- Cloud radiation interaction: Slingo (1987).

The surface boundary condition of sea surface temperature (SST) is obtained from the weekly blended SST of Reynolds and Smith (1994) and the soil moisture fields are obtained from a 2-yr climatology of the Global Soil Wetness Project (Dirmeyer and Zeng 1999). The snow cover was initialized from seasonally varying climatological data that are derived from seasonal albedo data. Carbon dioxide is assumed to be well mixed in both the models throughout the entire atmosphere with a constant value of 345 ppm.

The RSM model initially developed by Juang and Kanamitsu (1994) is used here. However, we have replaced the deep convection scheme [originally the simplified Arakawa–Schubert (SAS)] and the land surface processes (originally two-layer soil model of Mahrt and Pan 1984) in the RSM model with that of COLA AGCM, namely, RAS parameterization and Simplified Simple Biosphere Scheme (SSiB), respectively. As shown in our earlier study (Misra et al. 2002a) the implementation of SSiB has had a positive impact on the

TABLE 1. The details of model configuration.

Variable	RSM	AGCM
Horizontal resolution	80 km	T42 spectral truncation (312.5 km)
No. of vertical levels (same vertical discretization in both models)	18	18
Domain dimensions	217 × 112	128 × 64 (global)
Time step	240 s	600 s

RSM simulations. Furthermore, SSiB is a comprehensive land surface scheme. The reason for having identical convection schemes in the two models (COLA AGCM and RSM) is primarily to reduce the errors in the RSM simulations near the lateral boundaries. Our earlier experiments showed that for the same damping coefficients at the lateral boundaries the configuration with SAS as the convection scheme in RSM and RAS in COLA AGCM had far larger errors than that which involved the two models having identical convection schemes (not shown). Otherwise the results using RSM with RAS and SAS were similar in the interior of the domain. The rest of the RSM physics is briefly outlined below:

- Shortwave radiation: Chou et al. (1998);
- Longwave radiation: Fels and Schwarzkopf (1975);
- Boundary layer scheme: Miyakoda and Sirutis (1977);
- Vertical diffusion: Hong and Pan (1996);
- Shallow convection: Tiedtke (1984);
- Gravity wave drag parameterization: Alpert et al. (1988);
- Cloud–radiation interaction: Slingo (1987).

The horizontal resolution, the number of vertical levels, domain dimensions, and the time step of the two models are enumerated in Table 1. The vertical coordinate of both the models is the terrain-following sigma surface and the placement of the vertical levels are identical in both models.

In Figs. 1a and 1b we display the orography in the domain of the regional model from the AGCM and RSM, respectively. The relatively high-resolution orography in the RSM raises the height of the Andes Mountain by approximately 1000 m all along the western coast of South America. Furthermore, there is a improvement in the resolution of the orography in central America over Guatemala and Honduras. This increased height of the mountains in RSM also increases the horizontal gradient of the terrain relative to the AGCM. It should also be noted here that Fig. 1b also depicts the model domain of RSM.

3. Design of experiments

For this study we also chose the same time period as (Misra et al. 2002a,b) that is, January–February–March (JFM) of 1997, 1998, and 1999. For both the AGCM and RSM, five-member ensembles were integrated for each year. We produced a set of five 0000 UTC 15 December initial conditions for the AGCM for each year. To generate these initial conditions for the AGCM we first ran the model for a week using NCEP reanalyses of 0000 UTC 15 December of the corresponding year. We then reset the clock in the model restart file generated at the end of the (one week) model integration to the initial date to obtain a synoptically independent initial condition during essentially the same season. This was done recursively to obtain the other four initial conditions (Kirtman et al. 2001).

The RSM ensemble members were generated by initializing and forcing at 12-h intervals with each ensemble member of the AGCM. The surface boundary condition of sea surface temperature was identical in both models and was updated at 24-h intervals in the RSM runs. Both the models are integrated to 0000 UTC 1 April of the following year. The first 15 days of the integration are neglected for the analysis of the results to allow for spin up of the model.

4. Results

Here, we compare the ensemble mean results followed by a discussion of the intramember variance in the two models. The results are presented as a mean over all 15 seasonal simulations from each model including JFM of 1997, 1998, and 1999. The daily mean values were used to compute the seasonal mean of the model. A sample size of three years is too small to derive conclusive information on interannual variability that will, therefore, not be discussed in this paper. The observed seasonal climatology for JFM for various variables presented in the following sections are also computed over the same years (1997, 1998, and 1999).

a. Ensemble mean results

We compare the ensemble means of precipitation, circulation fields, and surface variables from the RSM and AGCM. The results are presented on the observational grid and, in the absence of observations, the fields are shown on the coarser model grid. The differences are computed on the coarser grid. However, the cross sections of the meridional jets are shown on the respective model grids.

1) PRECIPITATION

Figure 2 shows the precipitation from the COLA AGCM, observations from Xie and Arkin (1996) and the RSM. The observations are monthly mean values on a 2.5° latitude–longitude grid. On account of the higher resolution of the RSM relative to the observations and the AGCM, there are more finescale features in the mean precipitation shown in Fig. 2c. Contrary to observations the split intertropical convergence zone

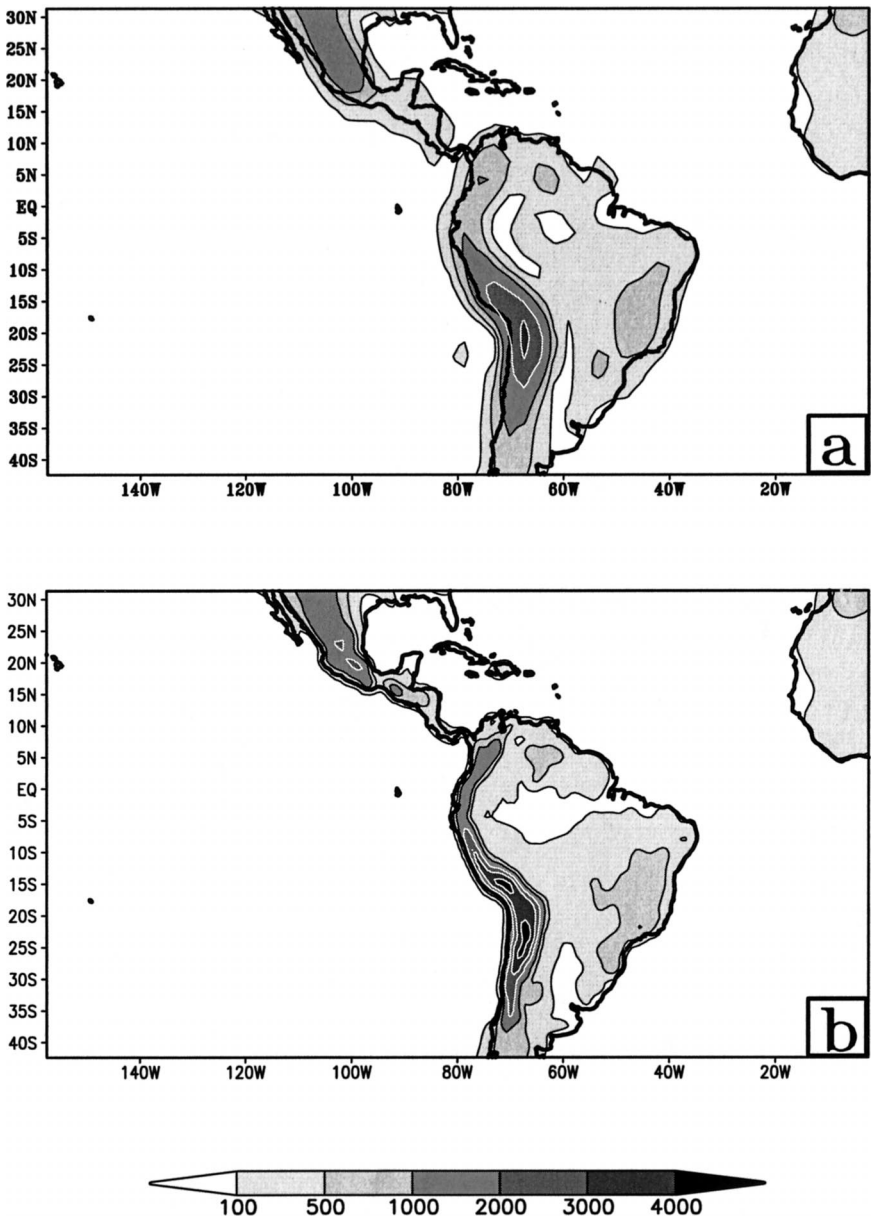

FIG. 1. Height of surface in m from (a) the AGCM and (b) the RSM. The contours are solid black lines up to 1000 m and are shaded light while the contours are white and shaded in dark beyond 1000 m.

(ITCZ) in both ocean basins is prevalent in the AGCM and RSM runs. The erroneously dry regions over Nordeste and the northern tip of South America (north of Llanos) are further exacerbated in the RSM. The RSM simulates more precipitation over the Amazon River basin (ARB), with the northern part of the river basin receiving in excess of 16 mm day^{-1}. However, the unrealistic dry areas over the central Amazon in the AGCM simulation is improved upon by the RSM. Furthermore, the increase in precipitation in the RSM simulation over the southeast Amazon and its southward extension to the South Atlantic convergence zone (SACZ) agrees well with the observations. The AGCM depicts unrealistically weak rain rates and has a banded structure in the region probably as a result of numerical instability arising from Gibbs phenomenon near the steep Andes mountains. The RSM improves the simulation over subtropical South America south of 20°S with increased precipitation in the range of 2–4 mm day^{-1} as opposed to near-dry conditions ($<$1 mm day^{-1}) in the AGCM simulation. The location of the northern branch of the ITCZ over the Atlantic Ocean is well simulated by both models. However, both models have an unrealistic tendency to develop a split ITCZ in both

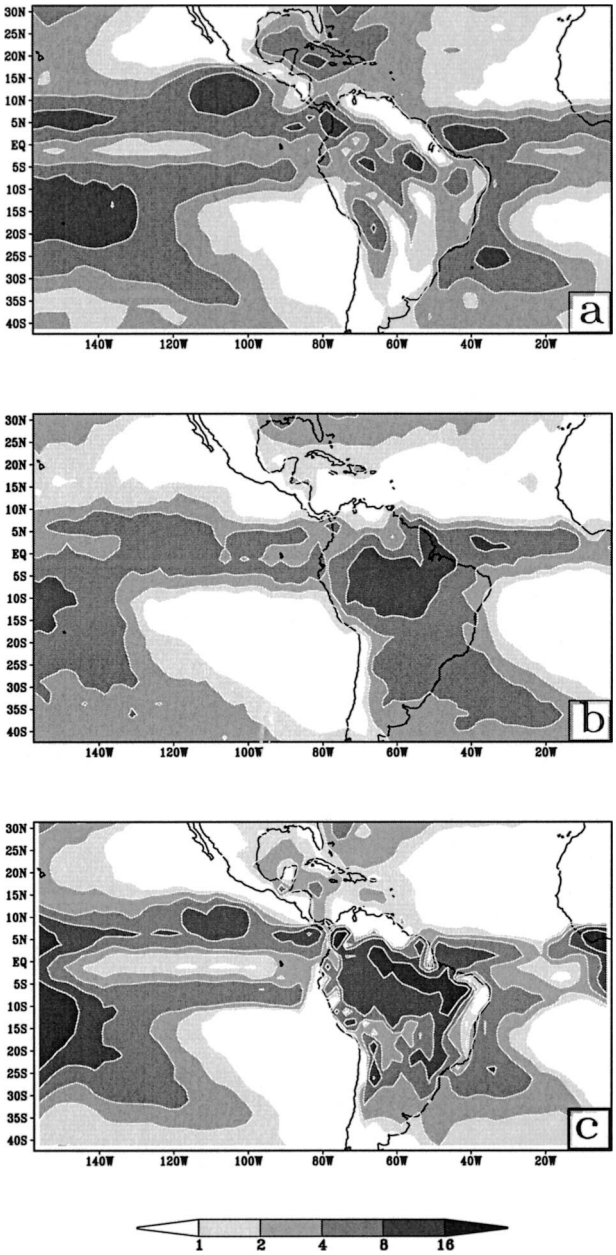

FIG. 2. Precipitation climatology for JFM from (a) the AGCM, (b) the observations, and (c) the RSM. The units are mm day^{-1}.

the Pacific and Atlantic Ocean basins. The extent of the dry subtropical zones over the ocean basins is greater in the RSM, which is more realistic than the AGCM simulations.

We have also examined the model results with a number of station observations over land from climate analysis monitoring system (CAMS) datasets that utilize rain gauge estimates (Janowiak and Xie 1999). Here, we show some of these comparisons that are representative of the Altiplano plateau, the southern Amazon basin, Nordeste (northeast Brazil), the SACZ (over land) and subtropical South America indicated by the following

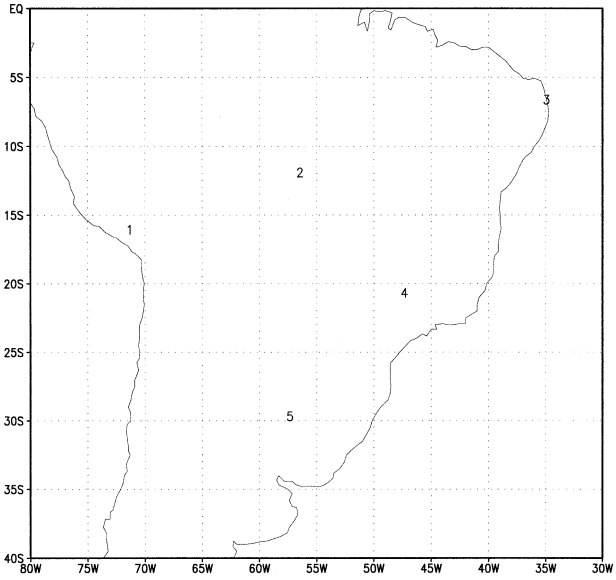

FIG. 3. The location of station observations used to compare model climatology.

stations: 1) Arequipa, Peru; 2) Vera, Argentina; 3) Natal, Brazil; 4) Franca, Brazil; and 5) Paso de los Libres, Argentina in Fig. 3, respectively. The comparison of the model JFM climatology precipitation and the corresponding observational climatology (computed over the same years as in the model simulation) over these five stations are shown in Table 2. As noted previously the Nordeste region is very dry in both models. Over the southern Amazon basin, SACZ, and subtropical South America both models tend to overestimate the mean JFM precipitation. However the RSM consistently improves over the AGCM over these areas, albeit quantitatively by a small amount. But the largest improvement by downscaling is seen over the Altiplano plateau. The AGCM simulates the mean JFM precipitation over this region in excess of 10 mm day^{-1} while the observations and the RSM results indicate nearly one-tenth of this value. This result may be attributed to the higher-resolution orography in the RSM that is able to resolve the plateau reasonably (Fig. 1b).

2) SUBSEASONAL VARIABILITY

The subseasonal variability is an important component of the region (Paegle and Mo 1997; Garreaud 1999;

TABLE 2. The comparison of the RSM and the AGCM precipitation climatology for JFM with station observations indicated in Fig. 3. The units are mm day^{-1}.

Station	Observations	RSM	AGCM
1	1.2	1.1	10.5
2	9.7	11.1	12.0
3	2.8	0	0.1
4	7.3	10.6	11.6
5	5.4	2.6	2.1

Liebmann et al. 1999). Liebmann et al. (1999) show that outgoing longwave radiation (OLR) fluctuations with periods less than 90 days have maximum variance in the SACZ and over subtropical South America in December–January–February (DJF). They further show that there is a local minimum in the variance over the southern Amazon basin, where mean convection is maximum. In addition, they find from correlations of submonthly OLR anomalies and 200-hPa streamfunction that the enhanced convection in the SACZ region at these scales occur at the leading edges of upper-level troughs propogating into the region from upper latitudes. Similarly, using observed OLR (Kousky and Casarin 1986; Paegle and Mo 1997) show a north–south dipole pattern with wet conditions over subtropical latitudes of South America when the SACZ is weak.

We examined the high-frequency (3–30 days) and the 30–40-day variance of the anomalies in OLR (not shown) in both the RSM and the AGCM. It was found that both models exhibit far less variance than the observations of Liebmann and Smith (1996). However, the RSM exhibited a relatively higher variance over subtropical South America, the SACZ, and the tropical Atlantic. These areas also showed a relative improvement in the seasonal mean precipitation in the RSM suggesting that these high temporal scales of variability contribute to the seasonal anomalies. But this result also suggests that the RSM simulations at 80-km horizontal resolution may still be inadequate to resolve these high-frequency oscillations.

A number of studies (Garreaud 1999; Lenters and Cook 1999) have shown significant variability of precipitation over Altiplano plateau and its correlation with large-scale circulation from intraseasonal to interannual scales. Garreaud (1999) showed that within the austral summer season of DJF, the wet spells over Altiplano were characterized by easterly wind anomalies in the mid- and upper troposphere and by westerly wind anomalies in the dry spell. These wind anomalies arise due to meridional shifts of the Bolivian high caused by variations in diabatic heating over the SACZ, the ARB, and the Altiplano plateau (Lenters and Cook 1999). This was examined in the RSM simulation as shown in Figs. 4a and 4b. Here, Fig. 4a is the daily zonal wind anomalies computed about the JFM climatology from the RSM runs, while Fig. 4b is the corresponding rainfall anomaly over an area between 15°–20°S and 70°–65°W. The RSM is able to reasonably pick the observed relationship between the precipitation and the prevalent wind anomalies in January and February. However, in March the model systematically simulates easterly anomalies through much of the troposphere despite negative anomalies of precipitation over the region. The AGCM barely had any variability (not shown) in precipitation over this region.

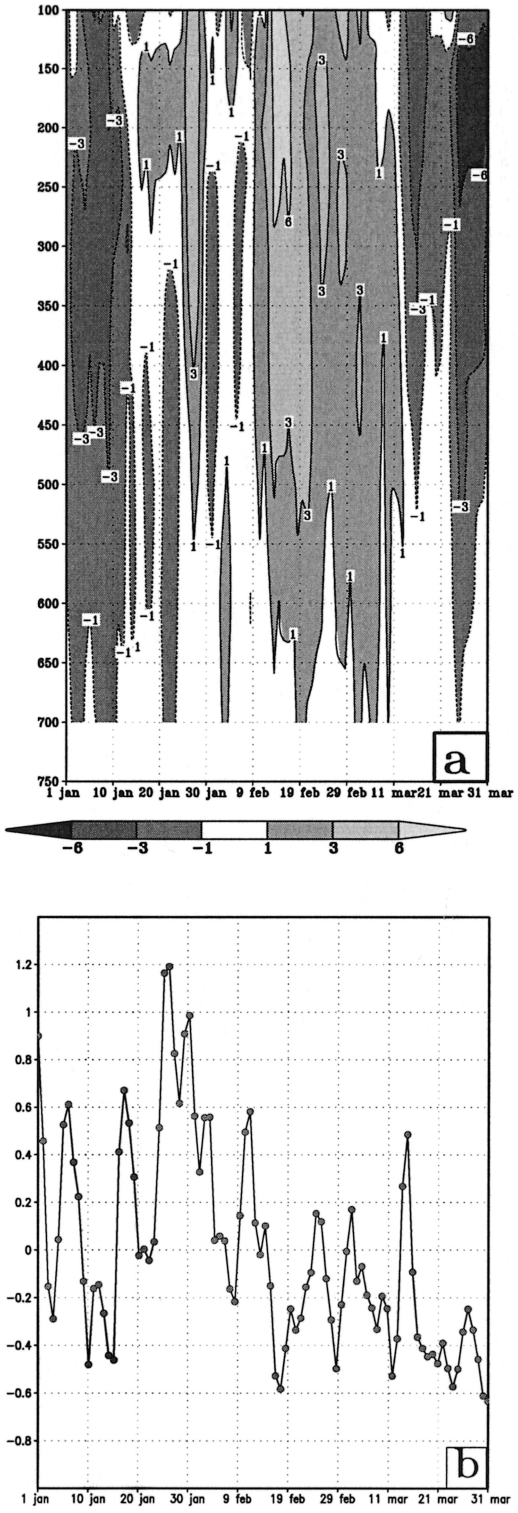

FIG. 4. The daily mean (a) zonal wind (m s^{-1}) and (b) precipitation (mm day^{-1}) anomalies from RSM over the Altiplano plateau.

3) LOW-LEVEL CIRCULATION

One of the most significant features of the low-level circulation over continental South America is the low-

level jet (LLJ) along the eastern slopes of the Andes, which is well documented in both observational (Douglas et al. 1998) and modeling studies (Misra et al. 2002b; Saulo et al. 1999). In Fig. 5 we show pressure–longitude cross sections of the meridional wind from the AGCM and the RSM at 25°S. Based on the observational study of Douglas et al. (1998), which included data from isolated in situ observations over Bolivia, it is seen that the core of the simulated LLJ in RSM is higher and far down south. The observations over eastern Bolivia (Douglas et al. 1998) indicate that the LLJ core is around 850 hPa and around 17°S. However, it should be noted that the LLJ is barely resolved at 80-km resolution, and the AGCM at T42 spectral truncation is not able to resolve the LLJ at all. The AGCM also produces an erroneous northerly wind maxima atop the Andes mountains at around 700 hPa. The NCEP reanalysis also displays a similar feature (not shown). The shallow northerly jet centered near the southeast coast of Brazil around 55°W (documented in Saulo et al. 1999) is also barely resolved by the RSM. These low-level circulation features are critical in determining the precipitation in subtropical South America. They serve as conduits of moisture supply from the Tropics to the subtropics. The uncertainities in these circulation features can cause discrepancies in the moisture budget over subtropical South America in excess of 50% (Wang and Paegle 1996). Wang and Paegle (1996) compared operational analyses and found that the principal sources of moisture budget discrepancies over subtropical South America are wind analysis uncertainity and vertical resolution.

4) SURFACE VARIABLES

In Fig. 6 we show the surface temperature simulated by the AGCM, observations at 300-km horizontal resolution (Ropelewski et al. 1985) and the RSM. It should be noted that the observational dataset of the surface temperature has been extended through 1999. The blank spaces over land in the observations indicate missing observations. The relatively warmer surface temperatures in the RSM over ARB is an improvement compared to the AGCM simulation. The warmer temperatures in the RSM over northeast Brazil also agree well with observations. However, the warm bias in the RSM over subtropical South America is accentuated compared to the AGCM simulation. Our previous study (Misra et al. 2002a) also showed a similar amplified warm bias in the RSM simulation forced by the NCEP reanalysis. It is interesting to note that despite the close proximity to the lateral boundaries where the RSM state variables are strongly relaxed toward the AGCM so-

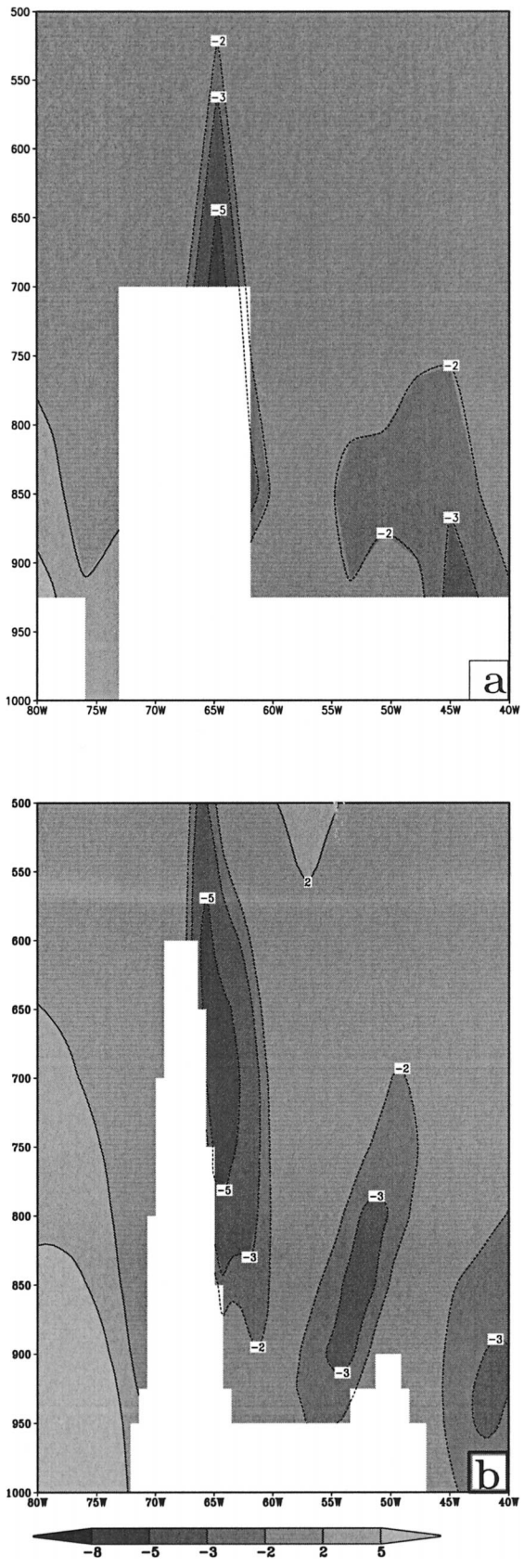

→

FIG. 5. The climatology of the meridional wind cross section at 25°S for JFM from (a) the AGCM and (b) the RSM. The units are m s^{-1}. The orography is shown in white.

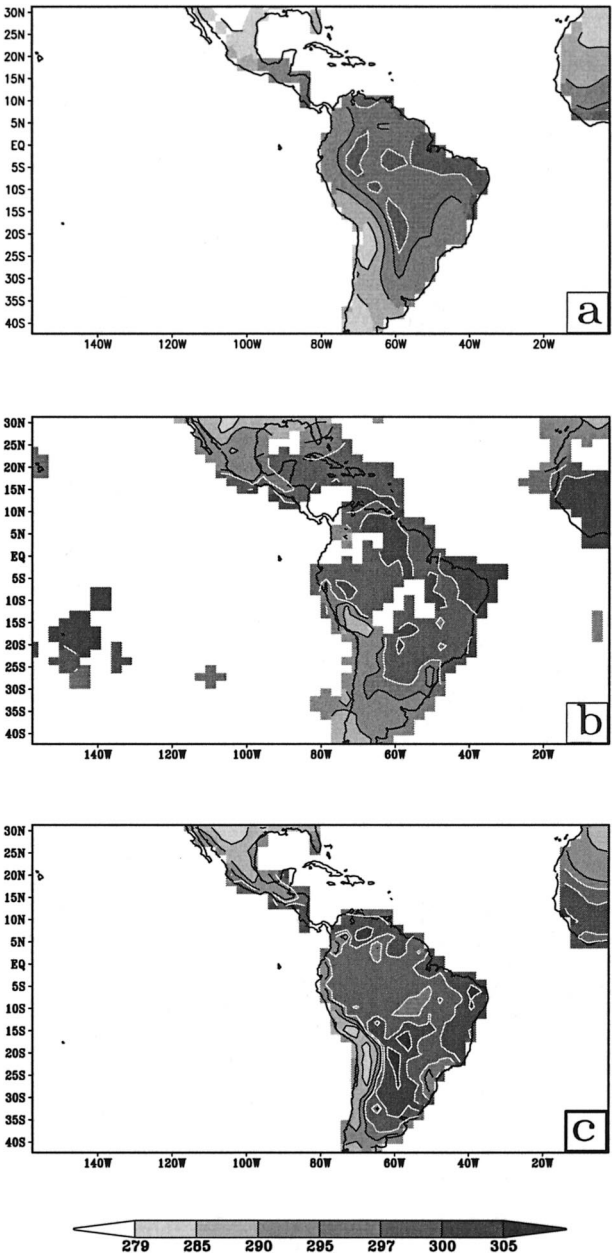

FIG. 6. The climatology of surface temperature for JFM from (a) the AGCM, (b) the observations, and (c) the RSM. The units are in K. Values up to (beyond) 295 K are shaded light (dark) and contoured in solid black (white) line. Blank spaces over land indicate missing observations.

lution, the West African surface temperatures in the RSM are much warmer and closer to the observations.

To further verify these results we made comparisons (Table 3) with station data over the points indicated in Fig. 3. The table shows that there is an improvement in the mean JFM surface temperature over Altiplano, Nordeste, and the SACZ region as noted in the large-scale analysis. However, over subtropical South America and the southern ARB the RSM deteriorates the warm bias observed in the AGCM.

TABLE 3. The comparison of the RSM and the AGCM surface temperature climatology for JFM with station observations indicated in Fig. 3. The units are °C.

Station	Observations	RSM	AGCM
1	15.2	14.2	16.5
2	26.4	23.3	25.3
3	28.2	30.3	33.1
4	23.4	24.3	27.1
5	24.8	30.8	29.7

Dirmeyer et al. (2000) in a intercomparison study showed that SSiB, unlike other land surface schemes has a tendency to partition the total energy at the surface with higher sensible and lower latent heat fluxes. It is seen from Figs. 7a and 7b that this bias in partitioning of total energy at surface is reduced slightly in RSM. Figures 7a and 7b show the difference in latent and sensible heat fluxes between the AGCM and the RSM, respectively. The RSM produces more latent heat flux than the AGCM by over 25 W m^{-2} in the ARB. Similarly the AGCM simulates higher sensible heat flux than the RSM over the ARB. Over subtropical South America the surface heat and moisture fluxes are comparable in the two models. Over the oceans especially over the eastern Atlantic Ocean, and Caribbean Sea, the AGCM simulates higher evaporative fluxes than the RSM.

b. Ensemble spread

As mentioned in the introduction, the degrees of freedom of RSM are limited because of the prescribed lateral boundary conditions from the COLA AGCM. Since the lateral boundaries for each ensemble member of the RSM simulation is prescribed from the corresponding ensemble member of the AGCM, one would expect the ensemble spread about the ensemble mean to have some correspondence in the two models. Furthermore, over the oceans the surface conditions in both models are identical, that is, observed SST is prescribed. Therefore, one might expect that the results of the integrations from the two models over the oceans will be closer to each other than that over land.

The standard deviation (SD) is computed as the square root of the variance about the ensemble mean that is calculated separately for each year and then averaged for all three years over the JFM season. To compare the ensemble spread between variables and between the two models we normalize this averaged standard deviation by the total standard deviation (TSD) to obtain the normalized standard deviation (NSD). The total standard deviation is obtained as the deviation about the climatological mean (average over all 15 simulations for each model). Mathematically, this may be expressed as

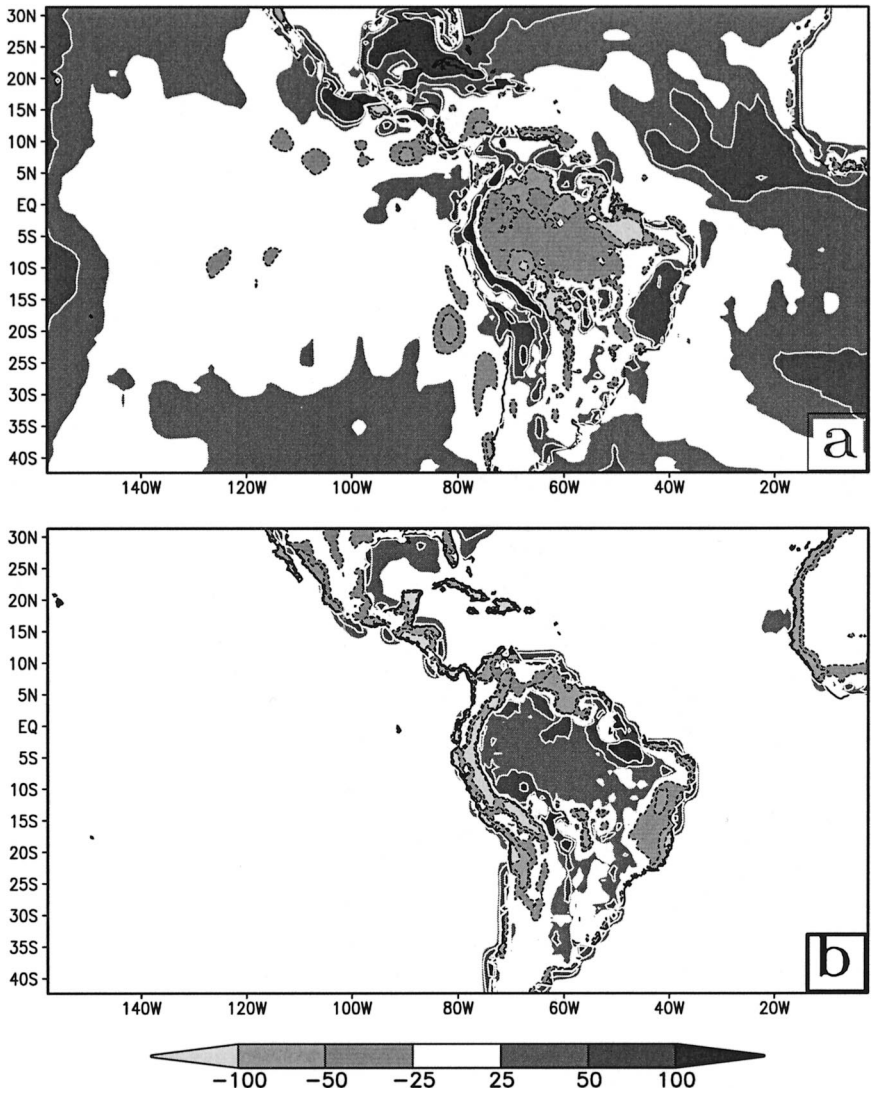

FIG. 7. The climatological difference between the AGCM and the RSM for JFM in (a) evaporative and (b) sensible heat flux. The units are W m^{-2}. Values below (above) -25 W m^{-2} are shaded light (dark) and contoured in dashed (solid) black (white) line.

$$\mathrm{SD} = \frac{1}{N}\sum_{i=1}^{N}\sqrt{\frac{1}{(n-1)}\sum_{j=1}^{n}(x_{ij}-\overline{x_i})^2}, \qquad (1)$$

where x_{ij} is the climate variable for N years ($i = 1, \ldots N$) and n ensemble members ($j = 1, \ldots n$). Here $\overline{x_i}$ is the ensemble mean. Then

$$\mathrm{TSD} = \sqrt{\frac{1}{N(n-1)}\sum_{i=1}^{N}\sum_{j=1}^{n}(x_{ij}-\overline{\overline{x}})^2}, \qquad (2)$$

where $\overline{\overline{x}}$ is the climatological (ensemble) mean defined as

$$\overline{\overline{x}} = \frac{1}{Nn}\sum_{i=1}^{N}\sum_{j=1}^{n}(x_{ij}). \qquad (3)$$

Finally,

$$\mathrm{NSD} = \frac{\mathrm{SD}}{\mathrm{TSD}}. \qquad (4)$$

This total standard deviation contains both the interannual signal and the internal variability (noise). Since we have a sample of just three years it is inappropriate to look at the interannual signal. However, with five ensemble members for each year, it is worthwhile to examine the intramodel variability (or model noise). It should be noted that a region with NSD of 1 indicates that the model noise is the dominating factor, while an NSD of 0 indicates total absence of model noise.

In Fig. 8 we show the difference in NSD of precipitation rate for the AGCM and RSM runs. It should be noted that while computing these differences the NSD of AGCM was linearly interpolated to the RSM grid. It

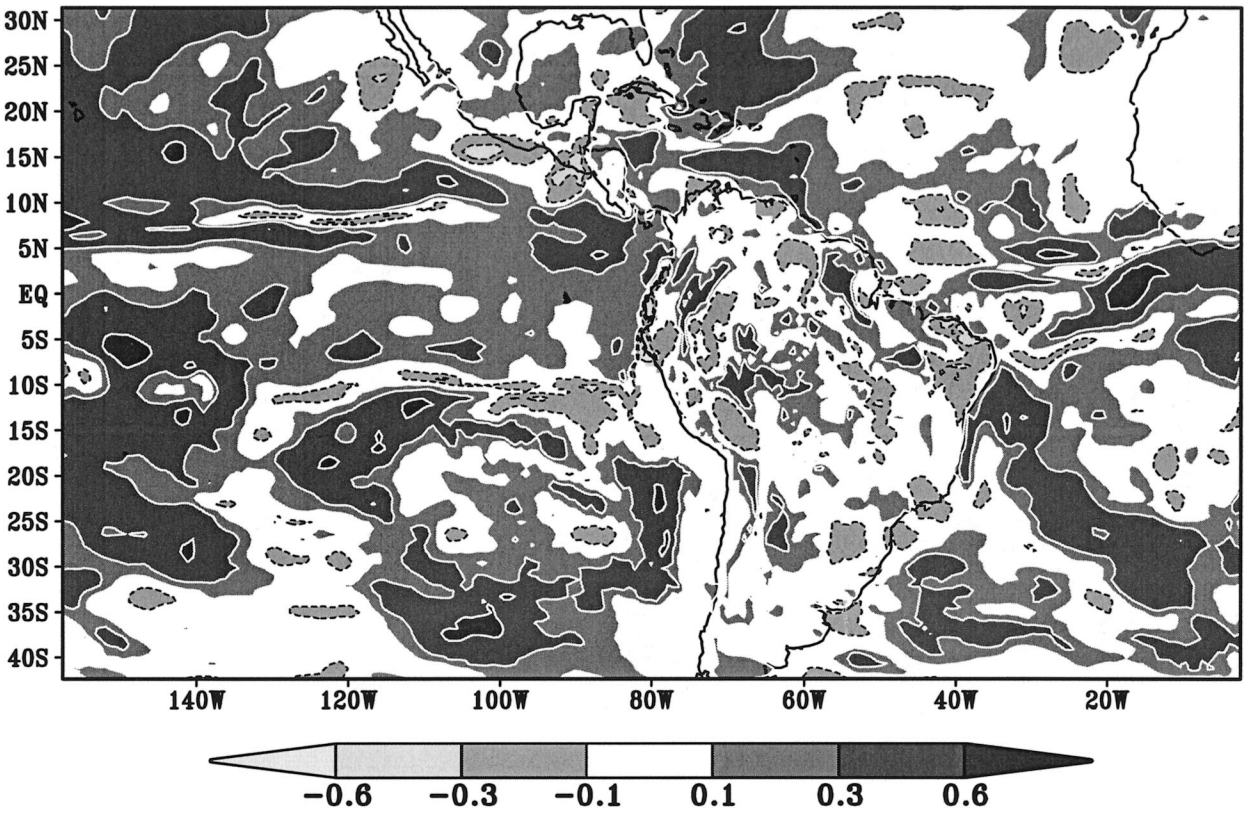

FIG. 8. Difference of the NSD of precipitation for JFM between the AGCM and the RSM. Values below (above) −0.1 are shaded light (dark) and contoured with dashed (solid) black (white) line.

is clearly seen from the figure that the model noise is greatly reduced over the ocean (particularly, the Pacific) and over certain regions of the ARB in the RSM simulation relative to the AGCM. This is intriguing because the large-scale variability in the RSM is forced by the AGCM and SST (which is identical in both models). This feature has also been observed with other regional climate models (A. Vernekar 2001, personal communication). In Fig. 9 the NSD of precipitation from RSM is shown, which indicates a high level of noise. This shows that the summer precipitation over this region is in large part unpredictable by the RSM and COLA AGCM as well (because the difference in the noise level between the two models is insignificant over land, see Fig. 8). The difference in the NSD of the surface fluxes are shown in Fig. 10. Similar to the precipitation, the model noise in evaporative (Fig. 10a) and sensible heat (Fig. 10b) fluxes over the oceans and over certain parts of the ARB are relatively smaller in the RSM runs. However, over other regions the intramodel variability is comparable between the two models.

The NSD of the low-level winds (Fig. 11) in the two models is the most similar among the variables examined. Unlike precipitation and surface fluxes, the noise in the low-level winds are remarkably similar over the oceans. It should be mentioned here that the flux computations over ocean are nearly identical in both models following Miyakoda and Sirutis (1977). There is, however, more noise displayed by the RSM over subtropical South America and northeast Brazil where the precipitation in Fig. 9 also showed considerable intramodel variability.

The difference in NSD of the surface temperature between the two models is shown in Fig. 12. The model noise in the surface temperature is comparable in both the models, consistent with the behavior of the surface fluxes over land shown earlier. Over central ARB, there is a significant reduction in the noise level in RSM compared to the AGCM. The soil moisture in the root zone (not shown) also showed a similar behavior.

It should be mentioned that the relatively high-resolution orography in RSM did not significantly change the predictability in the vicinity of the mountains except over the ARB in the variables examined here. However, in the mean the Andes Mountains in RSM did assist in the formation of a realistic LLJ and the resulting precipitation in the subtropical latitudes of South America.

In summary, the surface variables such as the precipitation and surface fluxes show far less intramodel variability over the oceans and parts of the ARB in the RSM simulations relative to the AGCM integrations. Over land, besides the ARB the variability in the two models is comparable. This study shows that the internal variability of the RSM in some variables is distinct from

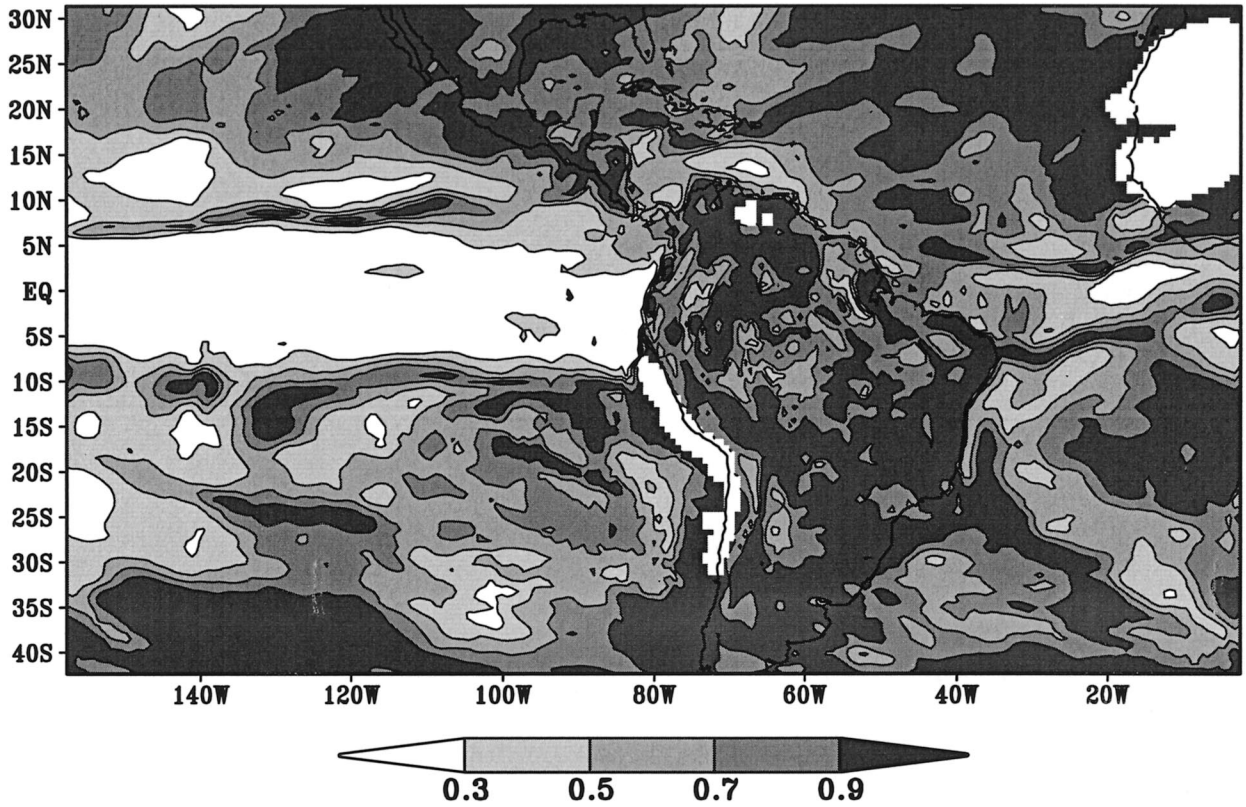

FIG. 9. NSD of precipitation for JFM from RSM.

that in the AGCM over the oceanic regions of the regional domain under consideration. It should be noted that there is more correspondence in the ensemble spread between the two models in winds and temperature (not shown) both over ocean and land. This is not surprising as these are prognostic variables of RSM, prescribed at the lateral boundaries by the AGCM. However, the surface variables, which have different ensemble spreads in the two models, are diagnostic quantities obtained as nonlinear functions of the prognostic variables implied in the physical parameterization schemes of the models. In other words the physics of the models are essentially causing the two models to diverge from each other. This occurs in spite of the fact that the two models use the same convective parameterizations. It may be that identical land surface parameterization (SSiB) in the two models may have resulted in comparable behavior of the intramodel variability of the diagnostic variables in the two models over land (except over the ARB). Over land, SSiB over this regional domain displays a certain resilience of predictability to variations in horizontal resolution as observed in the similarity of the intramodel variability of some of its state variables, such as surface temperature and soil moisture (not shown) and its diagnostic quantities like evaporative and sensible heat fluxes. Although there are significant differences in the mean characteristics of the two models (primarily due to differences in the resolution of orography), the comparable noise structures and magnitude over land calls for a certain resilience of predictability in SSiB to variations in horizontal resolution. This feature may be specific to the chosen regional domain. This remains to be explored further.

5. Conclusions

In this study we have compared the solutions from two models. The ensemble mean results show that the RSM is able to improve upon the climatology of the AGCM in many respects. The precipitation in the RSM over the SACZ, the ARB, and subtropical South America agrees better with observations than the COLA AGCM. However, it should be mentioned that the RSM does degrade the AGCM precipitation over the Nordeste region, the northern tip of South America, and persists the double ITCZ problem over both ocean basins. At the subseasonal scales the variance both at 3–30 and 30–60 days are improved in the RSM simulations over the SACZ and subtropical South America region. However, in general both models underpredict the variance at these subseasonal scales both over ocean and land. The surface temperature simulations are improved in the RSM over ARB but the warm bias is exacerbated over subtropical South America. The northerly jets along the eastern slopes of the Andes mountains and along the southeast coast of Brazil are barely resolved

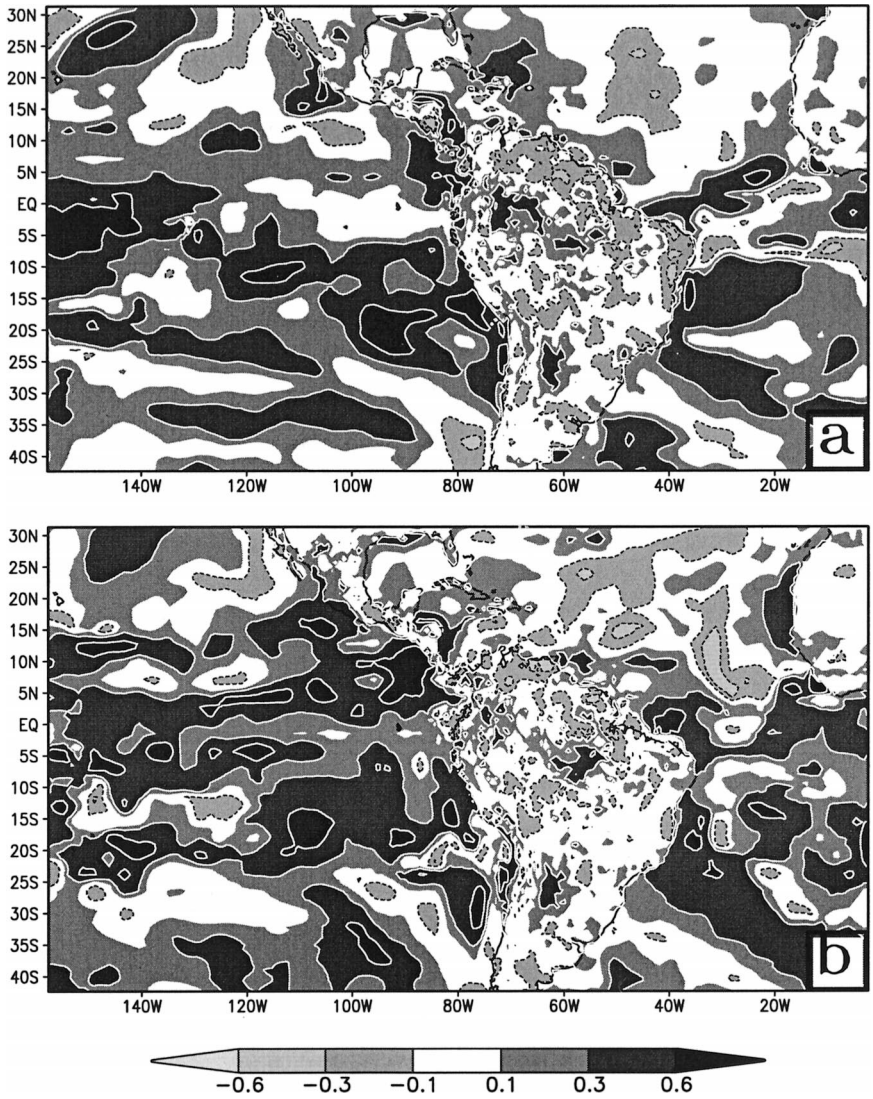

FIG. 10. Same as Fig. 8 but for (a) latent heat flux (LHF) and (b) sensible heat flux (SHF).

by the RSM, but absent in the AGCM. It should be mentioned that in this study the analysis of the models were conducted using coarse observational datasets that do not provide the high-frequency variability features to compare with the finescale features generated by the regional model. This problem is particularly accentuated over South America where the radiosonde network is very coarse. However, we showed comparisons of the two models with a few representative station observations that corroborate some of the conclusions. These comparisons at specific grid points also revealed that the RSM is able to make large improvements in the simulation of the mean JFM precipitation and surface temperature over the Altiplano plateau that may be related to the improved resolution of the orography in the model, which is able to resolve this plateau reasonably.

In this study we computed a normalized standard deviation (NSD) to compare and contrast the two models and to look into the relative variance between the variables of the same model. One of the important features that we find from the analysis of NSD in the two models is that the high-resolution orography in RSM did not make a noticeable difference in the predictability (or in the noise level) in the vicinity of the Andes Mountains from the AGCM except over parts of the ARB adjacent to the mountain. The NSD of the precipitation and surface fluxes are found to be smaller over the oceans and parts of the ARB in the RSM than in the AGCM. However, in the rest of the area over land the model noise is similar. This analysis also showed that the summer season precipitation over tropical and subtropical South America is highly unpredictable in both the RSM and the AGCM.

Generally the prognostic variables of the two models displayed similar intramodel variability. However, the noise level in diagnostic variables show significant dif-

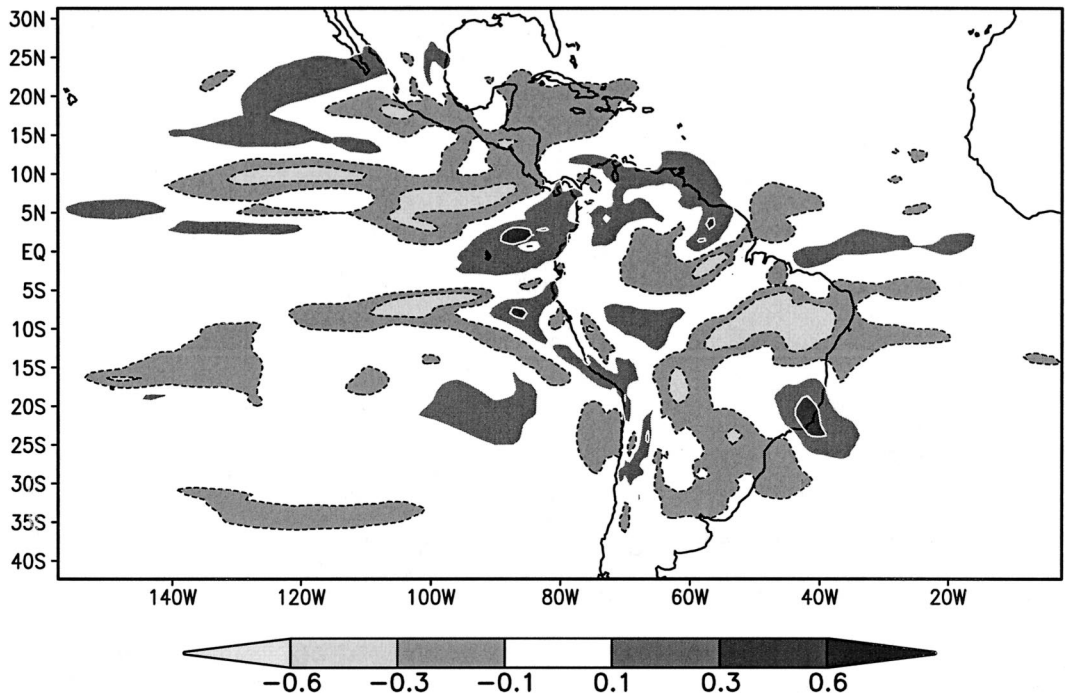

FIG. 11. Same as Fig. 8 but for 850-hPa wind speed.

ferences in the two models. Since the prognostic variables in the RSM are prescribed at the lateral boundaries by the AGCM, the degrees of freedom of these quantities are limited. Since the diagnostic quantities examined in this paper are nonlinear functions of the prognostic variables of the model, they show far different behavior in the intramodel variability of the two models. However, over land it is seen that the state variables of SSiB such as surface temperature and soil moisture (not shown) have comparable noise in the two models. Even

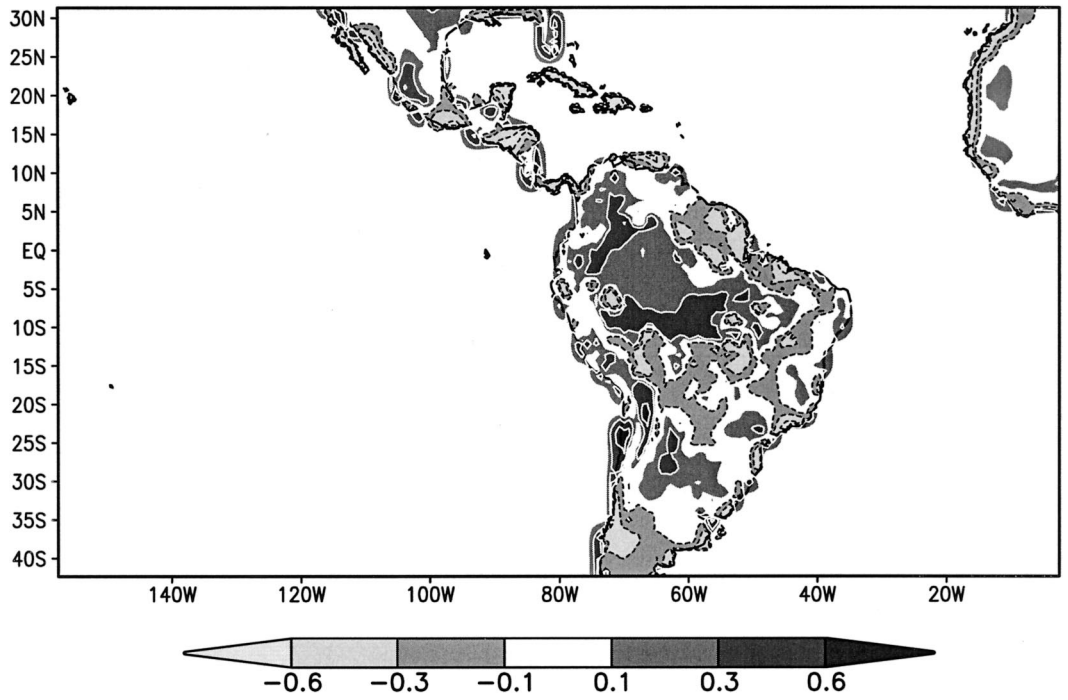

FIG. 12. Same as Fig. 8 but for surface temperature.

diagnostic quantities such as surface fluxes and precipitation display very similar intramodel variability in the two models over land. Although there are significant changes in the mean characteristics of the model simulations, similar noise structure and magnitude over most parts of the land area in the domain suggest a certain resilience of predictability in SSiB to variations in horizontal resolution. Considering the results of Giorgi and Bi (2000), which indicate that the internal variability in the regional climate can be modulated by the season of integration, the chosen model domain, and region of application, the current feature of reduced noise over oceans in the high-resolution runs of the RSM could also be a model-dependent result. This should be further explored by conducting many more experiments over other seasons and geographical regions as well.

Acknowledgments. This project was supported by NASA Grant NAG5-8416 and NOAA Grant NA86GP0258.

REFERENCES

Alpert, J. C., M. Kanamitsu, P. M. Caplan, J. G. Sela, G. H. White, and E. Kalnay, 1988: Mountain induced gravity drag parameterization in the NMC medium-range model. Preprints, *Eighth Conf. on Numerical Weather Prediction,* Baltimore, MD, Amer. Meteor. Soc., 726–733.

Chou, M.-D., M. J. Suarez, C.-H. Ho, M. M.-H. Yan, and K.-T. Lee, 1998: Parameterizations for cloud overlapping and shortwave single-scattering properties for use in general circulation and cloud ensemble models. *J. Climate,* **11,** 202–214.

Chou, S. C., A. M. B. Nunes, and I. F. A. Cavalcanti, 2000: Extended range forecasts over South America using the regional eta model. *J. Geophys. Res.,* **105,** 10 147–10 160.

Davies, R., 1982: Documentation of the solar radiation parameterization in the GLAS climate model. NASA Tech. Memo. 83961, 57 pp.

Dirmeyer, P. A., and F. J. Zeng, 1997: A two dimensional implementation of the Simple Biosphere (SiB) model. COLA Tech. Rep. 48, 30 pp. [Available from COLA, 4041 Powder Mill Road, Suite 302, Calverton, MD 20705.]

——, and ——, 1999: Precipitation infiltration in the simplified SiB land surface scheme. *J. Meteor. Soc. Japan,* **77,** 291–303.

——, ——, A. Ducharne, J. C. Morrill, and R. D. Koster, 2000: The sensitivity of surface fluxes to soil water content in three land surface schemes. *J. Hydrometeor.,* **1,** 121–134.

Douglas, M. W., N. Nicolini, and C. Saulo, 1998: Observational evidences of a low level jet east of the Andes during January–March 1998. *Meteorologica,* **3,** 63–72.

Fels, S. B., and M. D. Schwarzkopf, 1975: The simplified exchange approximation: A new method for radiative transfer calculations. *J. Atmos. Sci.,* **32,** 1475–1488.

Fennessy, M. J., and J. Shukla, 2000: Seasonal prediction over North America with a regional model nested in a global model. *J. Climate,* **13,** 2065–2627.

Figueroa, S. N., P. Satyamurty, and P. L. S. Dias, 1995: Simulations of the summer circulation over the South American region with an eta coordinate model. *J. Atmos. Sci.,* **52,** 1573–1584.

Garreaud, R. D., 1999: Multiscale analysis of the summertime precipitation over the central Andes. *J. Climate,* **12,** 901–921.

Giorgi, F., 1990: Simulation of regional climate using a limited area model nested in a general circulation model. *J. Climate,* **3,** 941–963.

——, and X. Bi, 2000: A study of internal variability of a regional climate model. *J. Geophys. Res.,* **105,** 29 503–29 521.

Harshvardhan, R. Davies, D. A. Randall, and T. G. Corsetti, 1987: A fast radiation parameterization for atmospheric circulation models. *J. Geophys. Res.,* **92** (D1), 1009–1016.

Hong, S.-Y., and H.-L. Pan, 1996: Nonlocal boundary layer vertical diffusion in a medium range forecast model. *Mon. Wea. Rev.,* **124,** 2322–2339.

Janowiak, J. E., and P. Xie, 1999: CAMS–OPI: A global satellite–rain gauge merged product for real-time precipitation monitoring applications. *J. Climate,* **12,** 3335–3342.

Ji, Y., and A. D. Vernekar, 1997: Simulation of the Asian summer monsoons of 1987 and 1988 with a regional model nested in a global GCM. *J. Climate,* **10,** 1965–1979.

Juang, H.-M., and M. Kanamitsu, 1994: The NMC nested regional spectral model. *Mon. Wea. Rev.,* **122,** 3–26.

——, S.-Y. Hong, and M. Kanamitsu, 1997: The NCEP regional spectral model: An update. *Bull. Amer. Meteor. Soc.,* **78,** 2125–2143.

Kiehl, J. T., J. J. Hack, G. Bonan, B. A. Boville, D. L. Williamson, and P. J. Rasch, 1998: The National Center for Atmospheric Research Community Climate Model: CCM3. *J. Climate,* **11,** 1131–1149.

Kinter, J. L., and Coauthors, 1997: The COLA Atmosphere–Biosphere General Circulation Model. Vol. 1: Formulation. COLA Tech. Rep. 51, 44 pp. [Available from COLA, 4041 Powder Mill Road, Suite 302, Calverton, MD 20705.]

Kirtman, B. P., D. A. Paolino, J. L. Kinter, and D. M. Straus, 2001: Impact of tropical subseasonal SST variability on seasonal mean climate simulations. *Mon. Wea. Rev.,* **129,** 853–868.

Kousky, V. E., and D. P. Casarin, 1986: Rainfall anomalies in southern Brazil and related atmospheric circulation features. *Extended Abstracts, Second Int. Conf. on Southern Hemisphere Meteorology,* Wellington, New Zealand, Amer. Meteor. Soc., 435–438.

Lacis, A. A., and J. Hansen, 1974: A parameterization for the absorption of solar radiation in the earth's atmosphere. *J. Atmos. Sci.,* **31,** 118–133.

Leith, C. E., 1974: Theoretical skill of Monte Carlo forecasts. *Mon. Wea. Rev.,* **102,** 409–418.

Lenters, J. D., and K. H. Cook, 1999: Summertime precipitation variability over South America: Role of the large-scale circulation. *Mon. Wea. Rev.,* **127,** 409–431.

Liebmann, B., and C. A. Smith, 1996: Description of a complete (interpolated) outgoing long-wave radiation dataset. *Bull. Amer. Meteor. Soc.,* **77,** 1275–1277.

——, G. N. Kiladis, J. A. Marengo, T. Ambrizzi, and J. D. Glick, 1999: Submonthly convective variability over South America and the South Atlantic convergence zone. *J. Climate,* **12,** 1877–1891.

Mahrt, L., and H.-L. Pan, 1984: A two layer model of soil hydrology. *Bound.-Layer Meteor.,* **29,** 1–20.

Marengo, J. A., B. Liebmann, V. E. Kousky, N. P. Filizola, and I. C. Wainer, 2001: Onset and end of the rainy season in the Brazilian Amazon basin. *J. Climate,* **14,** 833–852.

Mellor, G. L., and T. Yamada, 1982: Development of a turbulence closure model for geophysical fluid processes. *Rev. Geophys. Space Phys.,* **20,** 851–875.

Menendez, C. G., A. C. Saulo, and Z.-X. Li, 2001: Simulation of South American wintertime climate with a nesting system. *Climate Dyn.,* **17,** 219–231.

Misra, V., P. A. Dirmeyer, and B. Kirtman, 2002a: A comparative study of two land surface schemes in regional climate integrations over South America. *J. Geophys. Res.,* **107,** LBA 48.1–48.9.

——, ——, ——, H.-M. Juang, and M. Kanamitsu, 2002b: Regional simulation of interannual variability over South America. *J. Geophys. Res.,* **107,** LBA 3.1–3.16.

Miyakoda, K., and J. Sirutis, 1977: Comparative integrations of global spectral models with various parameterized processes of subgrid scale vertical transports. *Beitr. Phys. Atmos.,* **50,** 445–487.

Moorthi, S., and M. J. Suarez, 1992: Relaxed Arakawa–Schubert: A parameterization of moist convection for general circulation models. *Mon. Wea. Rev.,* **120,** 978–1002.

Nigam, S., and E. DeWeaver, 1998: Influence of orography on the extratropical response to El Niño events. *J. Climate,* **11,** 716–733.

Paegle, N., and K. C. Mo, 1997: Alternating wet and dry conditions over South America during summer. *Mon. Wea. Rev.,* **125,** 279–291.

Rao, V. B., C. E. Santo, and S. H. Franchito, 2002: A diagnosis of rainfall over South America during the 1997/98 El Niño Event. Part I: Validation of NCEP–NCAR reanalysis rainfall data. *J. Climate,* **15,** 502–521.

Reynolds, R. W., and T. M. Smith, 1994: Improved global sea surface temperature analyses using optimum interpolation. *J. Climate,* **7,** 929–948.

Ropelewski, C. F., J. E. Janowiak, and M. F. Halpert, 1985: The analysis and display of real time surface climate data. *Mon. Wea. Rev.,* **113,** 1101–1107.

Saulo, C., M. Nicolini, and S. C. Chou, 1999: Model characterization of the South American low level flow during the 1997–98 sprint summer season. *Climate Dyn.,* **16,** 867–881.

Schneider, E. K., 2001: Understanding differences between the equatorial Pacific as simulated by two coupled GCM's. COLA Tech. Rep. 98, 46 pp. [Available from COLA, 4041 Powder Mill Road, Suite 302, Calverton, MD 20705.]

Slingo, J. M., 1987: The development of verification of a cloud prediction scheme for the ECMWF model. *Quart. J. Roy. Meteor. Soc.,* **13,** 899–927.

Tanajura, C., 1996: Modeling and analysis of the South American summer climate. Ph.D. dissertation, University of Maryland at College Park, 164 pp.

Tiedtke, M., 1984: The effect of penetrative cumulus convection on the large-scale flow in a general circulation model. *Beitr. Phys. Atmos.,* **57,** 216–239.

Wang, M., and J. Paegle, 1996: Impact of analysis uncertainty upon regional atmospheric moisture flux. *J. Geophys. Res.,* **101,** 7291–7303.

Wilby, R. L., and T. M. L. Wigley, 1997: Downscaling general circulation mode output: A review of methods and limitations. *Prog. Phys. Geogr.,* **21,** 530–548.

Xie, P., and P. Arkin, 1996: Analyses of global monthly precipitation using gauge observations, satellite estimates, and numerical model predictions. *J. Climate,* **9,** 840–858.